Female Centered Mate Selections as an Explanatory Mechanism for Dimorphic Solutions in a Rock-Paper-Scissors Game

Abena S. B. Annor[1], Kelly R. Buch[2], Daniel A. Rodríguez-Pinzón[3], Michael R. Lin [4], Kamaldeen Okuneye [4], Benjamin R. Morin[4]

1 University of Florida, Gainesville, FL, USA

2 Southern Illinois University of Edwardsville, Edwardsville, IL, USA

3 Universidad de Los Andes, Bogotá, Colombia

4 Arizona State University, Tempe, AZ, USA

Abstract

Side-blotched lizards, *Uta stansburiana*, exhibit trimorphic male throat-colors (orange, blue, or yellow). In terms of mating, the males participate in an apparent game of rock-paper-scissors determined by throat color (i.e., a cyclic dominance chain). Mathematical models of this behavior predict stable monomorphic and trimorphic populations. However, researchers have observed stable dimorphic populations of orange and blue males. Furthermore, it is postulated that the only large-scale, long-term, stable solutions exclude the yellow throat type. We propose a new mathematical model accounting for the female population available for mating that may exhibits such behavior. We discuss the conditions under which particular population configurations are stable and flow attractive. We use these results to motivate conservative methods that may mitigate biodiversity loss by preventing the decline of a particular monomorphic or dimorphic population.

1 Introduction

Biodiversity is an important characteristic to the measurement of the health of ecological systems [6]. A biologically diverse system is better able to adapt to disruptive environmental changes [8]. Identifying the conditions under which an ecosystem undergoes a reduction in biodiversity is critical to the study of its conservation [10]. Non-hierarchical dominance

systems, in which no species or morph has complete dominance over all others, may maintain biodiversity [20]. Thus, exploring how specific examples of non-hierarchical dominance break down into hierarchical structures subject to massive population decline benefits the study of biodiversity.

One species that exhibits non-hierarchical dominance with respect to mating behavior is *Uta stansburiana*, a desert lizard native to Western North America, commonly known as the side-blotched lizard. Male side-blotched lizards exhibit three hereditary throat colors: oran(G)e, (B)lue, or (Y)ellow [17]. Each of the three male types has a reproductive advantage over one other male type but is inferior to the third [18]. Orange-throated males have the highest levels of testosterone and defend a large territory. They aggressively attack and drive off blue-throated lizards, who also hold territory, so orange-throated males can mate with females on both orange and blue territory. However, yellow-throated males, who do not defend territory, rely on their physical and behavioral similarity to females to easily infiltrate the relatively unmonitored orange territory and mate. Even though blue-throated males generally lose against orange-throated males in a head-on fight, they meticulously guard and track their females which prevents the yellow-throated males from easily sneaking into blue territory to mate with females. Since there is not a single dominant male morph (throat color), the fitness of a given morph is dependent on the prevalence of the others in a manner similar to a rock-paper-scissors (RPS) game [18].

Similarly, female *Uta stansburiana* have either yellow or orange throats. They occupy either the blue or orange-throated males' territory, and the inheritance of both the female and male throat colors follows a set of complex rules. The relative mating rates for various male and female color morphs have been suggested to be context dependent and may rely on aspects such as social environment, ecological conditions, or individual experience [1]. The overall reproductive success is therefore highly dependent on female mate selection and is negative frequency dependent. In essence, this means that the optimal mating strategy for females is to: (a) mate with yellow when orange is common; (b) mate with blue when yellow is common; and (c) mate with orange when blue is common. This is because when young lizards of the male type that beats the most common male type mature, they will be the most fit [16].

Side-blotched lizard populations have maintained male populations exhibiting all throat

colors (i.e., the GBY trimorphism) for millions of years across all regions [7]. This is consistent with the robust persistence of the coexistence equilibrium present in many mathematical models of three competing species [1, 11, 14, 15, 17]. It has recently been observed that some populations have destabilized and lost biodiversity giving rise to dimorphic (BG) and monomorphic (B or G) populations. Interestingly, dimorphic and monomorphic populations that include yellow-throated males have not been observed [7]. The repeated loss of the yellow morph suggests that the evolutionary stable state of the RPS strategies may destabilize over large spatial and temporal scales [7, 13]. These findings contradict the traditional RPS mathematical models that exhibit only monomorphic and trimorphic populations. A proposed hypothesis for the cause of destabilization of the GBY trimorphism is female positioning (whether in orange or blue territory) and her resulting selectivity in partner [7].

We seek to expand the scope of RPS mathematical modeling by proposing a traditional two-sex pair formation model with a mating consent function that accounts for female selection. We investigate two functional forms for this consent function: (1) a constant consent function representing relative preference and (2) a pseudo-spatial consent function representing female membership to specific male-type territories. Pair formation models have been used in many different contexts, mainly two-sex problems in demography and mixing problems in multi-type epidemic models [4, 9, 12]. We use a pair formation model with rapid-pairing dynamics to assess how female selection may drive the disappearance of the yellow morph from a trimorphic population.

In Section 2 we introduce the mathematical model and detail its base assumptions. In Section 3, we analyze the stability of equilibria of each system both analytically and numerically. Finally, we discuss our results and their biological significance in Section 4, and we provide further support for our numerical results with a brief analysis of a simplified version of our model.

2 Model Description

We consider a population differentiated by gender (with males differentiated by throat color)[1] encompassing classes of orange-throated males (G), blue-throated males (B), yellow-throated males (Y), and females (F). All lizards within a class are considered identical and homogeneously-mixed. These individuals may form a breeding pair distinguished by the male phenotype: orange-throated male and female (P_G), blue-throated male and female (P_B), and yellow-throated male and female (P_Y). Pairs are formed according to a mass action flow: males of type-i seek out females at rate S_i. Given an encounter between a mate-seeking male and a female, the success of such a pairing type is dependent on a female consent function C_i. Since mating is rapid (modeled via a pair separation rate parameter of σ_i), we assume that death does not occur for individuals while paired. The birth rates, r_i, account for both clutch size and the success rate for each new individual to reach reproductive age. Each clutch exhibits roughly equivalent sex differentiation and clutch size, so males and females are born at the same per capita rate regardless of their father's type (i.e., $\forall i \in \{G, B, Y\}$ $r_i = r$ and $r_F = r$) [21].

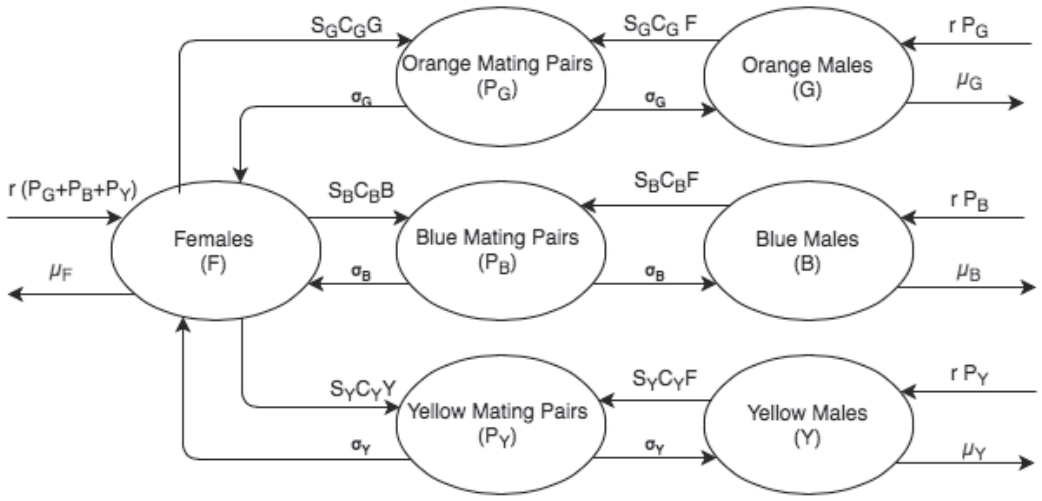

Figure 1: Flow to and from classes.

A seeking male of type-i attempts to court a female, and if successful, they form a

[1] We omit the female color dimorphism as a simplification meant to isolate the effect of availability akin to the survival of the weakest [11] and not confound the results with clutch viability considerations.

mating pair. After a mating event, one new, mature individual is immediately born into either the F class or male type-i class. Newborns are assumed to reach maturity instantly. A mating season realistically occurs during the summer, but we omit seasonality in our model by converting all rates to be in terms of the length of one mating season. Thus, events happen in a continuous time flow. Since there is not a limiting factor in the total population, the population size is able to grow without bound assuming that the landscape is arbitrary large enough to handle it. Therefore the density of lizards does not become supersaturated.

Using the flow depicted in Figure 1 and the parameters described in Table 1, we form the following system of differential equations to describe the mating dynamics of the side-blotched lizard:

$$\begin{aligned}
\frac{dG}{dt} &= (r+\sigma_G)P_G - \mu_G G - S_G G C_G F, \\
\frac{dB}{dt} &= (r+\sigma_B)P_B - \mu_B B - S_B B C_B F, \\
\frac{dY}{dt} &= (r+\sigma_Y)P_Y - \mu_Y Y - S_Y Y C_Y F, \\
\frac{dF}{dt} &= (r+\sigma_G)P_G + (r+\sigma_B)P_B + (r+\sigma_Y)P_Y - (S_G G C_G + S_B B C_B + S_Y Y C_Y + \mu_F)F, \\
\frac{dP_G}{dt} &= S_G G C_G F - \sigma_G P_G, \\
\frac{dP_B}{dt} &= S_B B C_B F - \sigma_B P_B, \\
\frac{dP_Y}{dt} &= S_Y Y C_Y F - \sigma_Y P_Y, \\
\frac{dN}{dt} &= \frac{dG}{dt} + \frac{dB}{dt} + \frac{dY}{dt} + \frac{dF}{dt} + 2\left(\frac{dP_G}{dt} + \frac{dP_B}{dt} + \frac{dP_Y}{dt}\right).
\end{aligned} \tag{1}$$

To study the effect of female selection, we consider two separate sets of rules for female consent to courting. Under our first assumption, we propose that female consent to mating with a particular male type is constant through time; thus, we set the consent as a fixed numerical value. These functions are best interpreted as unitless relative measures of female preference for specific male-types, reflecting the proportion of total mating attempts that are successful. Hence,

$$0 < C_i < 1.$$

Additionally, we propose a second set of non-constant consent functions to study how

Parameters	Unit	Biological Interpretation	Value [18, 21]
r	time^{-1}	birth rate of progeny that survive until maturity	1.094
μ_G	time^{-1}	death rate of orange males	1.229
μ_B	time^{-1}	death rate of blue males	1.075
μ_Y	time^{-1}	death rate of yellow males	1.075
μ_F	time^{-1}	death rate of females	0.956
S_i	lizard^{-1} time^{-1}	rate at which type-i males seek females	[20,60]
σ_i	time^{-1}	rate at which a P_i pair separates	18,864
ν_G	meter^2	territory defended by an orange male	100
ν_B	meter^2	territory defended by a blue male	40

Table 1: Model parameters with their biological definition and estimated value or range indexed by male throat color $i \in \{G, B, Y\}$. Time is measured in mating season.

the state of the current population affects the female's decision. In order to account for the disproportionate size of orange and blue territories, we propose a pseudo-spatial consent function where each male type is given a weight based on the territory they occupy and the control they exert over it.

$$\begin{aligned} C_G &= 1 \\ C_B &= \frac{\nu_B(B+P_B)}{\nu_G(G+P_G)+\nu_B(B+P_B)} \\ C_Y &= \frac{\nu_G(G+P_G)}{\nu_G(G+P_G)+\nu_B(B+P_B)} \end{aligned} \tag{2}$$

The total space occupied by the lizard population will be the sum of the space occupied by all the blue and orange-throated male lizards as yellows do not defend territory. In a system with any number of lizards, the mating events will always favor orange lizards because their physiology allows them to mate with their females and with females within blue territory. When the proportion of orange-throated males is high, the possibility of yellow-throated males to obtain multiple matings by sneaking into orange territory is higher (yellow beats orange) and that of blue-throated lizards is lower (orange beats blue). In the extreme case of a complete blue-throated male population, yellow-throated males cannot sneak into blue's territory (blue beats yellow). Assuming that ν_B and ν_G account for both the relative size of each color-morph's territory and the density of females therein, these consent functions represent the RPS game mediated through the preference of females.

3 Analysis and Results

In this section, we discuss the estimates of parameter values used in our analysis as well as our theoretical and numerical analysis performed on Model (1) with both Constant Consent and Pseudo-Spatial Consent Functions in order to determine stability of their equilibria. Due to the exponential and unbounded growth our model assumes, the population can approach infinity (Figure (2)). Under exponential growth, we consider the persistent population distribution (Figure (3)). We denote such Stable Population Distributions as SPD [5].

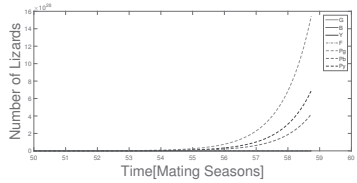

Figure 2: Exponential Growth.

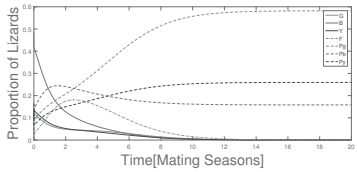

Figure 3: Stable Proportion Distribution.

3.1 Parameter Estimation

Since we model only the reproductive season, we use the time unit of one mating season for all parameters. We assume the average mating season to last 131 days, or 4.3 months [21]. The birth rate is estimated as the product of the average number of clutches per female per mating season, the average number of eggs per clutch, and percentage of hatchlings that survive to reproductive age per sex type. This yields an average birthrate of 1.094 new mature lizards of each gender type born to each female per mating season. Additionally, the seeking rates, a measure of how often a male seeks and finds a female whom he will court, must be estimated. In our numerical solutions, we estimate each seeking rate to be between 20 and 60 attempts per mating season roughly based off data presented in [21]. We consider seeking rates proportional to the activity of each male type as reported in [18], i.e., we as-

sume $S_Y < S_B < S_G$. Since mating lasts a very short time, our average pair separation rate should be very large [21]. Assuming a mating event lasts 10 minutes, then the separation rate is $18,864$ per mating season.

For the estimation of the death rates, we note that a several-year study of a population of side-blotched lizards found that generally there is a complete turnover of the mature population every year [21]. Since we consider new entries in our system to be mature adults aged to 8 months, we use 4 months as an average life span after reaching maturity. This results in an average death rate of 1.075 deaths per mating season. In our parameter estimation, we consider $\mu_F < \mu_B = \mu_Y < \mu_G$. This assertion is biologically significant as the high plasma testosterone level of orange-throated lizards reduces its lifespan [18]. Furthermore, females tend to live longer since they are protected by males [21]. In the absence of further data, we took the average lifespan of 4 months after maturation derived from [21] to apply to blue and yellow males, increased it by half a month for females, and decreased it by half a month for orange males. Additionally, the average home range of orange-throated males is about 100 square meters and that of blue-throated males to be about 40 square meters [18]. Thus, we use these values for ν_G and ν_B respectively. We assume females to be uniformly distributed among all area, so these also capture the average number of females on orange and blue-throated territory. A complete listing of all parameter values and their estimates can be found in Table 1.

3.2 Analysis of Model (1) with Constant Consent

Assuming Model (1) and phenomenological constant values for the consent functions are such that $0 < C_Y < C_B < C_G < 1$, the biologically relevant equilibrium states are given in Table 2. Four additional equilibria exist on the boundaries within our parameter space but they are not biologically relevant (See Appendix).

The Jacobian matrix for this case, $J_1(E^*)$ is given by:

Equilibrium $E_1{}^* = (G^*, B^*, Y^*, F^*, P_G^*, P_B^*, P_Y^*)$	Biological Interpretation	Stability
$E_{1_0} = (0,0,0,0,0,0,0)$	Extinction	Stable
$E_{1_G} = (\frac{\sigma_G \mu_F}{S_G C_G r}, 0, 0, \frac{\sigma_G \mu_G}{S_G C_G r}, \frac{\sigma_G \mu_F \mu_G}{S_G C_G r^2}, 0, 0)$	Monomorphic Orange	Saddle
$E_{1_B} = (0, \frac{\sigma_B \mu_F}{S_B C_B r}, 0, \frac{\sigma_B \mu_B}{S_B C_B r}, 0, \frac{\sigma_B \mu_F \mu_B}{S_B C_B r^2}, 0)$	Monomorphic Blue	Saddle
$E_{1_Y} = (0, 0, \frac{\sigma_Y \mu_F}{S_Y C_Y r}, \frac{\sigma_Y \mu_Y}{S_Y C_Y r}, 0, 0, \frac{\sigma_Y \mu_Y \mu_F}{S_Y C_Y r^2})$	Monomorphic Yellow	Saddle

Table 2: Equilibria of the Model (1) with constant consent functions. All equilibria exist under the assumption that all parameters are positive. All equilibria are initially evaluated at values in Table 1. If unstable, then we evaluated within a biologically relevant parameter space.

$$\begin{pmatrix} -C_G F S_G - \mu_G & 0 & 0 & -C_G G S_G & r+\sigma_G & 0 & 0 \\ 0 & -C_B F S_B - \mu_B & 0 & -C_B B S_B & 0 & r+\sigma_B & 0 \\ 0 & 0 & C_Y F S_Y - \mu_Y & -C_Y S_Y Y & 0 & 0 & r+\sigma_Y \\ -C_G F S_G & -C_B B S_B & -C_Y F S_Y & -C_G G S_G - C_B B S_B - C_Y Y S_Y - \mu_F & r+\sigma_G & r+\sigma_B & r+\sigma_Y \\ C_G F S_G & 0 & 0 & C_G G S_G & -\sigma_G & 0 & 0 \\ 0 & C_B F S_B & 0 & C_B B S_B & 0 & -\sigma_B & 0 \\ 0 & 0 & C_Y F S_Y & C_Y S_Y Y & 0 & 0 & -\sigma_Y \end{pmatrix}.$$

The Jacobian Matrix evaluated at the extinction equilibrium, E_{1_0}, has eigenvalues $-\sigma_G$, $-\sigma_B$, $-\sigma_Y$, $-\mu_G$, $-\mu_B$, $-\mu_Y$, and $-\mu_F$. Since all parameters are positive, the extinction equilibrium is locally asymptotically stable. Unfortunately, similar analysis on the monomorphic equilibria is currently intractable as eigenvalues are rather large. Thus, we calculate the eigenvalues for each monomorphic solution using our estimated biological parameter values from Table 1. The eigenvalues are described in Table 3.

Interestingly, each equilibrium value is inversely related to its associated consent parameter. That is, increasing C_i actually decreases the number of male type-i, P_i, and F at the type-i monomorphic equilibrium. Also, the first three eigenvalues for each monomorphic equilibrium are independent of the consent functions. This peculiarity motivates us to examine the specific subset of biological parameters over which each eigenvalue depends, seen in Table 4.

The stability of the extinction equilibrium is determined only by the death and divorce rates. Regardless of the seeking rate, the extinction equilibrium will remain stable. Likewise, the growth rate r does not affect the extinction equilibrium's stability. This means that for a population near the extinction equilibrium increasing growth and/or seeking rates can not

Calculated Equilibrium $(G^*, B^*, Y^*, F^*, P_G^*, P_B^*, P_Y^*)$	Eigenvalues: $e_1, e_2, e_3, e_{4,5}, e_{6,7}$
Monomorphic Orange $(\frac{364.32}{C_G}, 0, 0, \frac{468.36}{C_G}, \frac{407.05}{C_G}, 0, 0)$	$0.36 - 0.4e^{-4}i$ $-56336.23 - 1.87e^{-7}i$ $-1.08 + .36e^{-4}i$ $-\frac{0.1e^{-1}(8.81\times10^5 C_Y + 9.34\times10^5 C_G \pm \sqrt{8.72\times10^{11}C_G^2 + 1.65\times10^{12}C_G C_Y + 7.76\times10^{11}C_Y^2})}{C_G}$ $-\frac{0.1e-1(9.34\times10^5 C_G + 9.27\times10^5 C_B \pm \sqrt{8.72\times10^{11}C_G^2 + 1.73\times10^{12}C_G C_B + 8.59\times10^{11}C_B^2})}{C_G}$
Monomorphic Blue $(0, \frac{409.86}{C_B}, 0, \frac{460.88}{C_B}, 0, \frac{400.55}{C_B}, 0)$	$0.36 - 0.2e^{-4}i$ $-53695.18 - .15e^{-5}i$ $-1.01 + .31e^{-4}i$ $-\frac{0.11e^{-1}(7.71\times10^5 C_Y + 8.30\times10^5 C_B \pm \sqrt{6.89\times10^{11}C_B^2 + 1.28\times10^{12}C_B C_Y + 5.94\times10^{11}C_Y^2})}{C_B}$ $-\frac{0.11e^{-1}(9.13\times10^5 C_G + 8.30\times10^5 C_B \pm \sqrt{8.33\times10^{11}C_G^2 + 1.52\times10^{12}C_G C_B + 6.89\times10^{11}C_B^2})}{C_B}$
Monomorphic Yellow $(0, 0, \frac{431.44}{C_Y}, \frac{485.14}{C_Y}, 0, 0, \frac{421.63}{C_Y})$	$0.36 - 0.2e^{-4}i$ $-53695.18 - .23e^{-5}i$ $-1.01 + .32e^{-4}$ $-\frac{0.12e^{-1}(7.89\times10^5 C_Y + 9.13\times10^5 C_G \pm \sqrt{8.33\times10^{11}C_G^2 + 1.44\times10^{12}C_G C_Y + 6.22\times10^{11}C_Y^2})}{C_Y}$ $-\frac{0.12e^{-1}(7.89\times10^5 C_Y + 8.11\times10^5 C_B \pm \sqrt{6.58\times10^{11}C_B^2 + 1.28\times10^{12}C_B C_Y + 6.22\times10^{11}C_Y^2})}{C_Y}$

Table 3: Listing of eigenvalues corresponding to $J_1(E_{1_G})$, $J_1(E_{1_B})$, and $J_1(E_{1_Y})$ respectively evaluated at parameter values listed in Table 1. All numbers are rounded to two decimal places. Note: Let e_j be the jth eigenvalue of each equilibrium state as listed in the above table.

Eigenvalue Indices	Depend on
1,2,3	$\sigma_Y, \mu_F, \mu_G, \mu_B$, and μ_Y
4,5	$\sigma_Y, \sigma_G, S_Y, S_G, C_Y, C_G, \mu_Y, \mu_G$, and r.
6,7	$\sigma_Y, \sigma_B, S_Y, S_B, C_Y, C_B, \mu_Y, \mu_B$, and r

Table 4: Parameters on which each eigenvalue associated with the monomorphic yellow equilibrium depend.

save the population. This is biologically counter intuitive.

We next study the monomorphic equilibria and use the monomorphic yellow as an example without loss of generality. We find that the first three eigenvalues are dependent on μ_F, μ_Y, r, and σ_Y only; e_4 and its conjugate, e_5, depend on all Y and G parameters, and that e_6 and its conjugate, e_7, depend on all Y and B parameters. Stability is therefore determined by the comparative relationship between competitive male types and less on the female's ecology.

To further study e_1, e_2, and e_3, we sample the μ_F, μ_Y, r, and σ_Y parameter space to

determine parameter values that would make e_1, e_2, and e_3 all have non-positive real part. Parameter sweeps indicate that the real part of each eigenvalue is negative only when the parameters are allowed to be negative. Thus, we exclude the possibility of a biologically relevant stable equilibrium. Studying eigenvalues, e_4, e_5, e_6, and e_7, we find that oscillatory behavior of solutions only occur if C_Y and C_G and if C_Y and C_B have opposite signs which is not biologically plausible. We also find that when e_4 and e_6 are negative that e_5 and e_7 are positive. Therefore, the monomorphic yellow equilibrium point is classified as an unstable saddle point for all parameter choices.

Accordingly, when at the equilibrium point for a given parameter set, a negative perturbation of C_Y (i.e., a small decrease in C_Y) results in Y, F and P_Y populations asymptotically decreasing to zero (Figure 4a). Conversely, with a positive perturbation of C_Y (i.e., a small increase in C_Y), the Y and F populations remain relatively constant but the P_Y population exponentially increases (Figure 4b). Thus, the total Y-male population persists though almost exclusively as part of a mating pair. Perturbations of the other consent values, C_G and C_B, do not affect the population dynamics near the monomorphic yellow equilibrium.

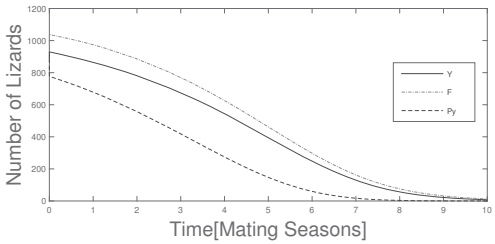

(a) Negative perturbation of C_Y when at equilibrium yields decreasing yellow male population.

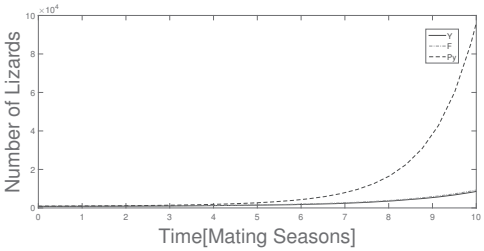

(b) Positive perturbation of C_Y when at equilibrium yields increasing yellow male population.

Figure 4: Monomorphic yellow population vs. time. Plot a and b result from a decrease and increase of an equilibrium consent value ($C_Y = .5$) respectively. The same population dynamics are observed in the monomorphic orange and monomorphic blue equilibria.

Interestingly, introducing a certain number of an additional male type into a declining monomorphic population prevents the population from asymptotically decreasing to zero. Without the additional male type, the population declines but with the additional male type, pairs of both types persist at SPD (Figure 5). This occurs even when the new male population introduced is less than the original number of resident type-i males. The final SPD of the dimorphism depends on the relation between the invading and resident states consent values (Figure 6). Likewise, it is possible to revive a declining orange-blue dimorphisim by introducing yellow which leads to a trimorphic population in the SPD.

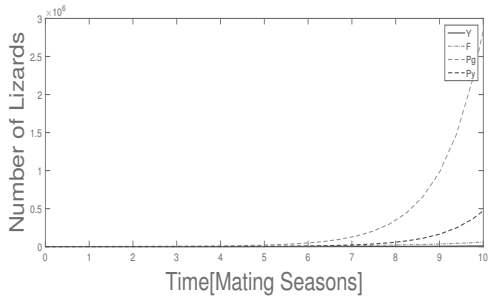

(a) Total yellow-male population increases as total population increases.

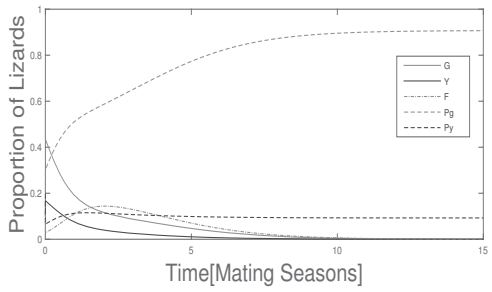

(b) Proportion of total yellow male population increases and stabilizes at SPD

Figure 5: The introduction of 1700 orange males into the declining monomorphic yellow population seen in Figure 4a revives the population. Similar dynamics are observed in the blue and orange monomorphic states.

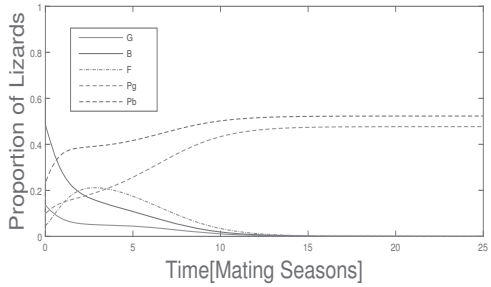

(a) Blue revives orange with $C_B = .3$ and maintains a higher proportion than orange.

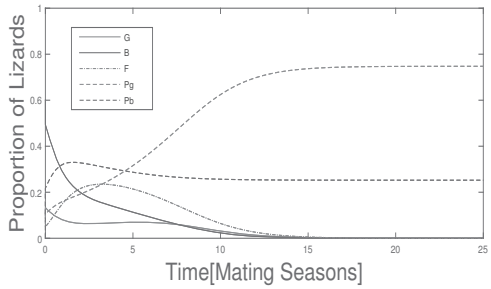

(b) Blue revives orange with $C_B = .25$ and maintains a smaller proportion than orange.

Figure 6: 5000 blues revive an asymptotically decreasing orange population. Depending on relationship between consent values, we get different dimorphic SPD.

3.3 Analysis of Model (1) with Pseudo-Spatial Consent

Supposing Model (1) and consent functions described by System (3), we have equilibria of the form found in Table 5.

Equilibrium ${E_2}^* = (G^*, B^*, Y^*, F^*, P_G^*, P_B^*, P_Y*)$	Biological Interpretation	Stability
$E_{2_0} = (0, 0, 0, 0, 0, 0, 0)$	Extinction	Stable
$E_{2_G} = (\frac{\mu_F \sigma_g}{rS_g}, 0, 0, \frac{\mu_g \sigma_g}{rS_g}, \frac{\mu_F \mu_g \sigma_g}{r^2 S_g}, 0, 0)$	Monomorphic Orange	Unstable
$E_{2_B} = (0, \frac{\mu_F \sigma_B}{rS_B}, 0, \frac{\mu_B \sigma_B}{rS_B}, 0, \frac{\mu_F \mu_B \sigma_B}{r^2 S_B}, 0)$	Monomorphic Blue	Unstable
$E_{2_{GB}} = (\frac{L}{rS_G K}, -\frac{H}{rK}, 0, \frac{\mu_g \sigma_g}{rS_g}, \frac{L}{r^2 S_g K}, -\frac{H}{r^2 K}, 0)$	Dimorphic Orange-Blue	Unstable

Table 5: Equilibria of the Pseudo-Spatial Model where $L = \nu_B \mu_F \mu_g^2 \sigma_g (rS_g \mu_B \sigma_B + S_g \mu_B^2 \sigma_B - rS_B \mu_g \sigma_g - S_B \mu_B \mu_g \sigma_g)$, $H = \nu_g \mu_B \mu_F \mu_g (r + \mu_g) \sigma_B \sigma_G$, and $K = -rS_G \nu_G \mu_B^2 \sigma_B + rS_G \nu_B \mu_B \mu_G \sigma_B + S_G \nu_B \mu_B^2 \mu_G \sigma_B - S_G \nu_G \mu_B^2 \mu_G \sigma_B - rS_B \nu_B \mu_G^2 \sigma_G - S_B \nu_B \mu_B \mu_G^2 \sigma_G$. All equilibria are initially evaluated at values in Table 1. If unstable, then we evaluated within a biologically relevant parameter space.

The Jacobian matrix for this case at the extinction equilibrium is given by:

$$J_2(E_{2_0}) = \begin{pmatrix} -\mu_G & 0 & 0 & 0 & r+\sigma_G & 0 & 0 \\ 0 & -\mu_B & 0 & 0 & 0 & r+\sigma_B & 0 \\ 0 & 0 & -\mu_Y & 0 & 0 & 0 & r+\sigma_Y \\ 0 & 0 & 0 & -\mu_F & r+\sigma_G & r+\sigma_B & r+\sigma_Y \\ 0 & 0 & 0 & 0 & -\sigma_G & 0 & 0 \\ 0 & 0 & 0 & 0 & 0 & -\sigma_B & 0 \\ 0 & 0 & 0 & 0 & 0 & 0 & -\sigma_Y \end{pmatrix}. \tag{3}$$

Since all eigenvalues are always negative, the extinction equilibrium is locally asymptotically stable. Now, we analyze the orange monomorphic equilibrium via the Jacobian matrix evaluated at E_{2_G}:

$$J(E_{2_G}) = \begin{pmatrix} -\mu_G - \frac{\mu_G\sigma_G}{r} & 0 & 0 & -\frac{\mu_F\sigma_G}{r} & r+\sigma_G & 0 & 0 \\ 0 & -\mu_B & 0 & 0 & 0 & r+\sigma_B & 0 \\ 0 & 0 & -\mu_Y - \frac{S_Y\mu_G\sigma_G}{rS_G} & 0 & 0 & 0 & r+\sigma_Y \\ -\frac{\mu_G\sigma_G}{r} & 0 & \frac{S_Y\mu_G\sigma_G}{rS_G} & -\mu_F & r+\sigma_G & r+\sigma_B & r+\sigma_Y \\ \frac{\mu_G\sigma_G}{r} & 0 & 0 & \frac{\mu_F\sigma_G}{r} & -\sigma_G & 0 & 0 \\ 0 & 0 & 0 & 0 & 0 & -\sigma_B & 0 \\ 0 & 0 & \frac{S_Y\mu_G\sigma_G}{rS_G} & 0 & 0 & 0 & -\sigma_Y \end{pmatrix}. \tag{4}$$

It is clear that $-\sigma_B$ and $-\mu_B$ are eigenvalues of $J(E_{2_G})$. Thus, it can be reduced to the

following five by five matrix:

$$A = \begin{pmatrix} -\mu_G - \frac{\mu_G \sigma_G}{r} & 0 & -\frac{\mu_F \sigma_G}{r} & r + \sigma_G & 0 \\ 0 & -\mu_Y - \frac{S_Y \mu_G \sigma_G}{r S_G} & 0 & 0 & r + \sigma_Y \\ -\frac{\mu_G \sigma_G}{r} & \frac{S_Y \mu_G \sigma_G}{r S_G} & -\mu_F & r + \sigma_G & r + \sigma_Y \\ \frac{\mu_G \sigma_G}{r} & 0 & \frac{\mu_F \sigma_G}{r} & -\sigma_G & 0 \\ 0 & \frac{S_Y \mu_G \sigma_G}{r S_G} & 0 & 0 & -\sigma_Y \end{pmatrix}. \tag{5}$$

Unfortunately, the remaining eigenvalues are intractable, so we must rely on numerical analysis. In a similar manner, $J_2(E_{2_B})$ has two obvious negative eigenvalues, $-\sigma_Y$ and $-\mu_Y$; it can be reduced to a five by five matrix with difficult eigenvalues. The stability analysis of the orange-blue dimorphic equilibrium results in a very large Jacobian matrix, and all seven eigenvalues are intractable. Thus, we proceed to numerical solutions to determine the stability of the monomorphic orange, monomorphic blue, and dimorphic orange-blue population.

For simplicity, we fix the parameters which are well reported in literature and vary the seeking (S_i) and pair separation rate (σ_i) as we do not have specific data for those values. We also vary the parameters which appear in the Jacobian to see their effect on stability of equilibria. We take equally distributed samples from sufficiently large ranges (i.e., $S_i \in (20, 60), \nu_B \in (1, 10), \nu_G \in (5, 15)$ and $\sigma_i \in (12500, 25000)$). Based on this numerical sweep, we conclude that all non-extinction equilibria are unstable for all biologically relevant parameters. This instability is mainly due to the exponential growth the model assumes. We proceeded to study the behavior of the SPD by varying both parameters and initial conditions. To better understand the stability of our equilibria, we sample the space of initial conditions surrounding an equilibrium point and simulate the resulting dynamics. We sample initial conditions (G_0, P_{G0}, F_0) from a cube surrounding the monomorphic orange equilibrium. We find that there exists a plane which intersects the equilibrium and separates space into two basins of attraction: initial conditions which lead to extinction and those that lead to exponential growth.

Our numerical solutions show the dimorphic population of yellow and orange males,

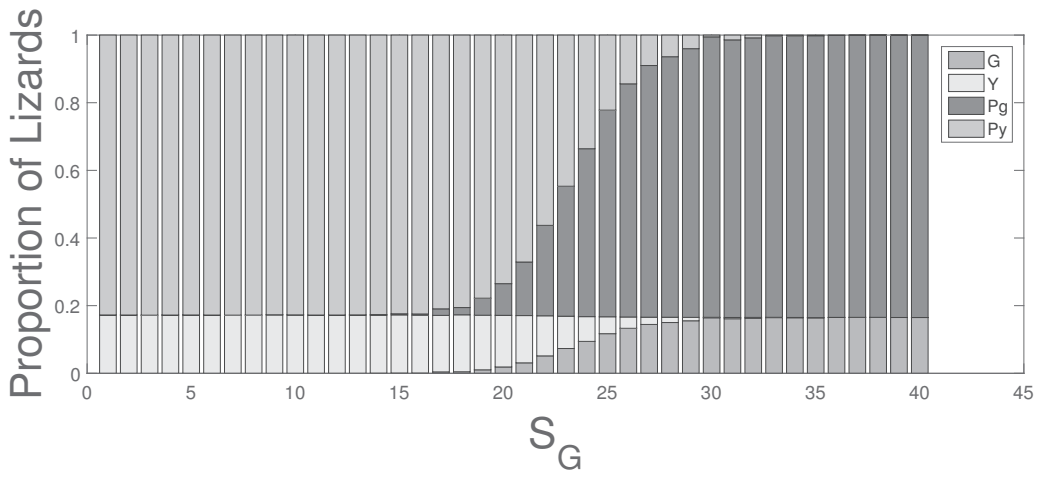

Figure 7: The effect of varying the seeking rate on the SPD at an orange-yellow dimorphic population. $\frac{G+Y}{P_G+P_Y}$ remains constant regardless of seeking rate.

which is not seen in nature [7]. We study this SPD by varying the seeking rate of orange lizards at the orange-yellow dimorphic coexistence (Figure 7). We find that as the seeking rate of orange increases, the SPD evolves from a monomorphic yellow population to a dimorphic orange-yellow population to finally a monomorphic orange population. Interestingly, we find that the ratio of the population in mating pairs to those in single classes stays constant regardless of seeking rate.

In order to study the effect of territoriality, we vary the ratio $\frac{\nu_B}{\nu_G}$ at the orange-blue dimorphic equilibrium (Figure 8). Because of the high seeking rate and female consent function of orange lizards, the system is unbalanced towards the orange morph. Thus, it requires a large ratio of blue initial population to reach the equilibrium. Increasing this ratio drives the population from monomorphic orange in the SPD to monomorphic blue in the SPD to complete extinction. This last effect can be explained because the aggregate consent function is not sufficient for the population to produce enough offspring. The ratio of $\frac{\nu_B}{\nu_G}$ given in Table 1 drives the population to an orange monomorphic population in the SPD.

In a fashion similar to the basic reproductive number of an epidemiological model, we study invasion threshold of dimorphic equilibria such that an introduction of the third morph leads to trimorphic coexistence (Figure 9). We find that a small introduction of yellow males

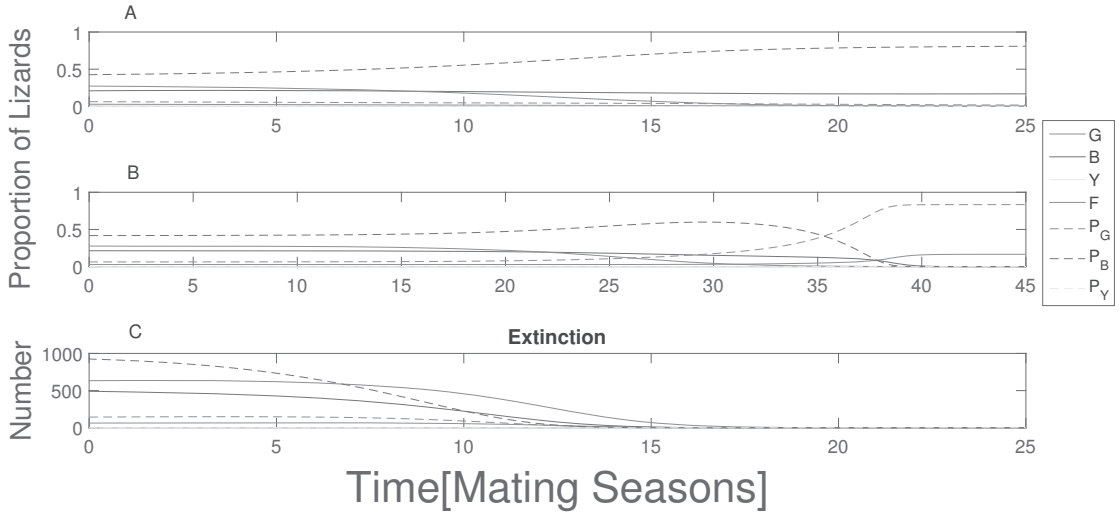

Figure 8: Effect of varying ν_G while at orange-blue coexistence in the pseudo-spatial model. Three possibles results are displayed: A. Dominance of the blue strategy, $\nu_B/\nu_G = 0.50$. B. Overcome and dominance of the orange strategy, $\nu_B/\nu_G = 0.40$. C. Total Extinction of the population,. $\nu_B/\nu_G = 0.33$..

into a dimorphic orange-blue population perturbs the system such that orange becomes dominant in the SPD. However, a large introduction of yellow induces a cyclic RPS dominance wherein yellow dominates the population originally but eventually, due to female selection, yellow relegates dominance to blue. Soon after, orange dominate over blue but finally, since yellow beats orange, yellow becomes the dominant morph again. Here, our numeric solver breaks down due to the extreme size of our state variables, but we can extrapolate that this cyclic dominance would continue over time.

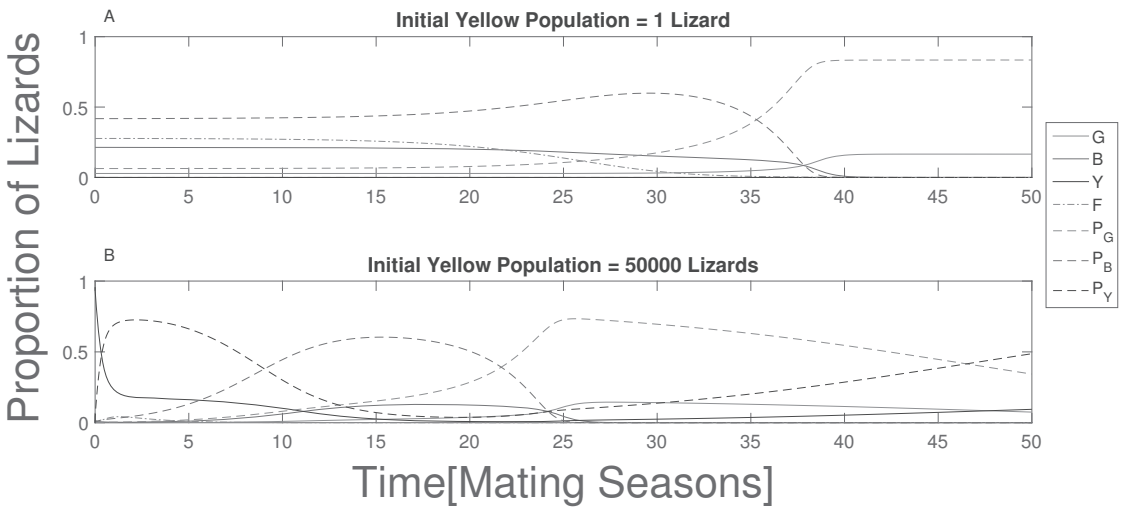

Figure 9: Long term effect on the population after the introduction of yellow lizards in the system. In B, we see cyclic dominance of the three male morphs. Here, C_G=0.75 to favor the blue side and have a more realistic scenario.

4 Discussion

Previous approaches to modeling the population dynamics of side-blotched lizards have considered a male-only RPS dynamic. Although these models exhibit the oscillations in the population distribution observed in nature, they neglect the interaction between the male and female lizards. Some prominent researchers have suggested that female mate selection is one of the mechanisms that has destabilized the non-hierarchical dominance [2,3,7]. We used a pair formation framework to analyze some of the effects of female selection on population dynamics. By the mere fact that we employed a pair formation model, we have implicitly modeled the competition between the three strategies in forming mating pairs. The rock-paper-scissors dynamics are modeled via a consent function that determines the success of a given strategy. This consent may be constructed to model female selection as function of the state variables of the system, the environment and/or spatial factors. We find that the constant consent functions (not dependent on any state variables) provide no novel results beyond trimorphic coexistence and monomorphic dominance, nor it exhibits transient dynamics. In response we include pseudo-spatial consent functions that measure both territory size and female density in an average sense. Because our state variables are merely single

lizard and/or pairs of lizards currently mating, we fail to explicitly model the truer dynamics of male lizard's harems (that they maintain more than one female as a mating partner at a time). We approximate this by differentiating mate seeking and pair dissolution rates, but this may only serve at best as an average. Because we abstract maturation and the anestrus/estrus cycle of the organism, we allow for highly unrealistic mating regimes (e.g., a single individual mating with every member of the opposite sex within a single mating season). This contributes to the rapid increase of the population size. To deal with such growth, we attempt to analyze the Stable Population Distributions (SPD), which represents the stable proportion of the population, rather than the population counts themselves [5]. However, our choice of consent functions severely limit this endeavor.

We first proposed to model a scenario where females could have a predisposition to a specific male type with payoffs of specific male-morph strategies independent of the current population distribution. The SPD resulting from this constant consent function is a direct reflection of the relative consent values. In a sense this permitted us to study the case where male fitness to the environment is given solely by the other system parameters and not the population composition. The constant consent function is insufficient to replicate the RPS dynamics observed in the lizard population. We find the constant consent function's failure to support the idea that female selection is context dependent. Interestingly, we find that the introduction of a new type of lizards could alter the course of the system and save a specific morph from extinction. We explain this phenomenon via a scenario where a dying population is saved by the introduction of a better suited morph that maintains the female population in a range that allows the two morphs to coexist.

We also analyzed pseudo-spatial consent functions which exhibit short-term RPS dynamics. These functions account for the relative dominance of a certain male lizard within different territories. The pseudo-spatial consent function assumes that female lizards will mate with orange lizards in all cases because of their dominance over their own territory and their ability to drive blue males away. This process drives the population to an orange dominance which then leads to a yellow dominance due to the increase in females who will consent to mate with them. At this point the dynamics deviate from traditional models and are driven by the aggregate effect of the higher seeking rate, despite the shorter average life span, of orange lizards. A blue dominance is not a possible scenario unless there is an

extremely high initial population of blue males.

Due to the complexity of the Model (1) coupled with the high degree of non-linearity induced by the Pseudo-Spatial Consent functions in Equation System (3), we propose a slightly simpler model that may give us insights to the qualitative behavior of the more complex model. Formally, this may be constructed by allowing the pair separation rates to go to infinity (that the average duration a pairing lasts is 0 time and in a sense they do not exist). This omission of pairs in the system is modeled by:

$$\begin{aligned}
\frac{dG}{dt} &= rS_G GC_G F - \mu_G G, \\
\frac{dB}{dt} &= rS_B \frac{\nu_B B}{\nu_B B + \nu_G G} BF - \mu_B B, \\
\frac{dY}{dt} &= rS_Y \frac{\nu_G G}{\nu_B B + \nu_G G} YF - \mu_Y Y, \\
\frac{dF}{dt} &= rF\left(S_G GC_G + \frac{\nu_B B}{\nu_B B + \nu_G G} S_B B + \frac{\nu_G G}{\nu_B B + \nu_G G} S_Y Y\right) - \mu_F F. \qquad (6)
\end{aligned}$$

This system exhibits orange monomorphic, blue monomorphic, orange-blue dimorphic, and extinction equilibria. We find all equilibria to be unstable except the extinction equilibrium. These analytic results support our numeric results of Model (1). The full analysis of Model (6) can be found in 5.1 in the Appendix.

As a future extension of this research, further consent functions could be considered to represent additional biological characteristics that may play a role in female mate selection, such as density dependence. In general, we have missed the effect of r and K strategies displayed by the female side-blotched lizards [19]. This model could also be extended to distinguish between female types to explore this dynamic. Furthermore, this model would greatly benefit from a restructuring to include a carrying capacity to inhibit exponential growth. Finally, it would be interesting to perform a sensitivity analysis on our system to determine which parameters are most important in the dynamics of our system.

Overall, we found that female consent can explain the destabilization of trimorphic populations into dimorphic populations overtime. Additionally, we explored a few conservation efforts that can be used to maintain biodiversity where still present or reintroduce biodiversity where the system has already destabilized into dimorphic or monomorphic populations.

5 Appendix

5.1 Pseudo-Spatial Model Reformulation

Model (6) straightforwardly exhibits monomorphic solutions for G and B and a dimorphic solution for BG. This system does not have a monomorphic yellow equilibrium because yellow males are dependent on orange males to maintain females within their territory. With some subtle difficulty it can be shown that the system also exhibits an extinction equilibrium (Table 6).

Equilibrium ${E_3}^* = (G^*, B^*, Y^*, F^*)$	Biological Interpretation	Stability
$E_{3_0} = (0, 0, 0, 0)$	Extinction	Stable
$E_{3_G} = (\frac{\mu_F}{rS_G}, 0, 0, \frac{\mu_G}{rS_G})$	Monomorphic Orange	Unstable
$E_{3_B} = (0, \frac{\mu_F}{rS_B}, 0, \frac{\mu_B}{rS_B})$	Monomorphic Blue	Unstable
$E_{3_{GB}} = \left(P, Q, 0, \frac{\mu_G}{S_G r}\right)$	Dimorphic Orange-Blue	Unstable

Table 6: Equilibria of the Pseudo-Spatial Model Reformulation where P=$\frac{\nu_B \mu_F \mu_G (S_B \mu_G - S_G \mu_B)}{rS_G(S_B \nu_B \mu_G^2 + S_G \mu_B(\nu_G \mu_B - \nu_B \mu_G))}$ and Q=$\frac{\nu_G \mu_B \mu_F \mu_G}{r(S_G \nu_G \mu_B^2 - S_G \nu_B \mu_B \mu_G + S_B \nu_B \mu_G^2)}$. Note: These are not SPD equilibria.

The Jacobian matrix of the system evaluated at the extinction equilibrium, E_{3_0}, is given by:

$$J_3(E_{3_0}) = \begin{pmatrix} -\mu_G & 0 & 0 & 0 \\ 0 & -\mu_B & 0 & 0 \\ 0 & 0 & -\mu_Y & 0 \\ 0 & 0 & 0 & -\mu_F \end{pmatrix}. \tag{7}$$

It is clear that the extinction equilibrium of the reformulated model is also locally asymptotically stable (just like the extinction equilibrium of Model (1)) because eigenvalues are simply the entries on the main diagonal. The Jacobian matrix of the system evaluated at the monomorphic orange equilibrium is given by:

$$J_3(E_{3_G}) = \begin{pmatrix} 0 & 0 & 0 & \mu_F \\ 0 & -\mu_B & 0 & 0 \\ 0 & 0 & \frac{S_Y \mu_G}{S_G} - \mu_Y & 0 \\ \mu_G & 0 & \frac{S_Y \mu_G}{S_G} & 0 \end{pmatrix}, \tag{8}$$

with eigenvalues $-\mu_B, -\sqrt{\mu_G \mu_F}, \sqrt{\mu_G \mu_F}$, and $\frac{S_Y \mu_G}{S_G} - \mu_Y$. The first two are always negative, the third is always positive. The last is negative if $\frac{S_Y}{S_G} < \frac{\mu_Y}{\mu_G}$. Regardless of the sign of the fourth eigenvalue, the equilibrium is an unstable saddle. The Jacobian at monomorphic blue equilibrium is given by:

$$J_3(E_{3_B}) = \begin{pmatrix} \frac{\S_G \mu_B}{S_B} - \mu_G & 0 & 0 & 0 \\ \frac{\nu_G \mu_B}{\nu_B} & 0 & 0 & \mu_F \\ 0 & 0 & -\mu_Y & 0 \\ \frac{(S_G \nu_B - S_B \nu_G) S_B \mu_B}{\nu_B} & \mu_B & 0 & 0 \end{pmatrix}, \tag{9}$$

with eigenvalues $-\mu_Y, -\sqrt{\mu_B \mu_F}, \sqrt{\mu_B \mu_F}$, and $\frac{S_G \mu_B}{S_B} - \mu_G$. The first two are always negative, the third is always positive, and the fourth is negative when $\frac{S_B}{S_G} > \frac{\mu_B}{\mu_G}$. Just as in the orange monoporphic equilibrium, the blue monomorphic equilibrium is unstable.

The Jacobian evaluated at the orange-blue dimorphic equilibrium, $E_{3_{GB}}$, is:

$$\begin{pmatrix} 0 & 0 & 0 & \mu_F - \frac{S_G \nu_G \mu_B^2 \mu_F}{S_B \nu_B \mu_G^2 + S_G \mu_B (\nu_G \mu_B - \nu_B \mu_G)} \\ -\frac{S_G \nu_G \mu_B^2}{S_B \nu_B \mu_G} & \mu_B - \frac{S_G \mu_B^2}{S_B \mu_G} & 0 & \frac{S_G \nu_G \mu_B^2 \mu_F}{S_B \nu_B \mu_G^2 + S_G \mu_B (\nu_G \mu_B - \nu_B \mu_G)} \\ 0 & 0 & \frac{S_Y (\mu_G - \mu_B)}{S_G} - \mu_Y & 0 \\ -\frac{S_G \nu_G \mu_B^2}{S_B \nu_B \mu_G} + \mu_G & \mu_B (2 - \frac{S_G \mu_B}{S_B \mu_G}) & \frac{S_Y (\mu_G - \mu_B)}{S_G} & 0 \end{pmatrix}. \tag{10}$$

The most straight forward eigenvalue of this matrix is $\frac{S_Y (\mu_G - \mu_B)}{S_G} - \mu_Y$. This is negative under the assumption $\frac{S_Y}{S_G} < \frac{\mu_Y}{\mu_G + \mu_B}$. Thus, we can reduce our system to the following three by three matrix to continue determining the stability of this equilibrium:

$$A = \begin{pmatrix} 0 & 0 & \mu_F - \frac{S_G \nu_G \mu_B^2 \mu_F}{S_B \nu_B \mu_G^2 + S_G \mu_B (\nu_G \mu_B - \nu_B \mu_G)} \\ -\frac{S_G \nu_G \mu_B^2}{S_B \nu_B \mu_G} & \mu_B - \frac{S_G \mu_B^2}{S_B \mu_G} & \frac{S_G \nu_G \mu_B^2 \mu_F}{S_B \nu_B \mu_G^2 + S_G \mu_B (\nu_G \mu_B - \nu_B \mu_G} \\ -\frac{S_G \nu_G \mu_B^2}{S_B \nu_B \mu_G} + \mu_G & \mu_B (2 - \frac{S_G \mu_B}{S_B \mu_G}) & 0 \end{pmatrix}. \quad (11)$$

We now may apply Routh-Hurwitz criteria for three dimensional systems to the resulting characteristic polynomial. One condition for stability is that the determinant of matrix A must be positive. $Det(A) = \mu_B \mu_F (S_G \mu_G - S_B \mu_B) > 0$ implies $\frac{S_B}{S_G} > \frac{\mu_B}{\mu_G}$. Another condition for stability is that the trace must be negative. However, $Tr(A) = \mu_B - \frac{S_G \mu_B^2}{S_G \mu_G} < 0$ implies $\frac{S_B}{S_G} < \frac{\mu_B}{\mu_G}$. Thus, the meeting of one condition implies the failure of another. This is sufficient to show that the Dimorphic Orange-Blue Equilibrium is unstable without examining the other conditions of the Routh-Hurwitz criteria.

Thus, we show analytically that the extinction equilibrium is the only stable equilibrium of the Reformulated Pseudo-Spatial model, and all monomorphic and dimorphic equilibria are unstable saddles. This gives us confidence in our numerical results from the Model (1).

5.2 Derivation of Boundary Equilibria

Model (1) with constant consent parameters has four additional boundary equilibria not included in our main analysis. The derivation of the Orange-Blue Dimorphic Equilibria follows.

Assume $G \neq 0, P_G \neq 0, B \neq 0, P_B \neq 0$, and $F \neq 0$. Let $Y = 0$ and $P_Y = 0$. Setting the derivative of all state variables equal to zero yields:

$$\begin{aligned} 0 &= (r + \sigma_G) P_G - \mu_G G - S_G G C_G F, & (12) \\ 0 &= (r + \sigma_B) P_B - \mu_B B - S_B B C_B F, & (13) \\ 0 &= (r + \sigma_G) P_G + (r + \sigma_B) P_B - (S_G G C_G + S_B B C_B + \mu_F) F, & (14) \\ 0 &= S_G G C_G F - \sigma_G P_G, & (15) \\ 0 &= S_B B C_B F - \sigma_B P_B. & (16) \end{aligned}$$

Solving (15) for GF and substituting it into (12) gives

$$P_G = \frac{\mu_G}{r} G. \tag{17}$$

Likewise, solving (16) for BF and substituting it into (13) gives

$$P_B = \frac{\mu_B}{r} B. \tag{18}$$

Now, substituting (17) and (18) into (21) and (13) respectively yield

$$0 = \left[(r+\sigma_G)\frac{\mu_G}{r} - \mu_G - C_G S_G F\right] G \text{ and} \tag{19}$$
$$0 = \left[(r+\sigma_B)\frac{\mu_B}{r} - \mu_B - C_B S_B F\right] B. \tag{20}$$

Since we assume $G \neq 0$ and $B \neq 0$, (19) and (20) have one root each which exist when

$$F = \frac{\mu_G \sigma_G}{r S_G C_G} \text{ and} \tag{21}$$
$$F = \frac{\mu_B \sigma_B}{r S_B C_B}. \tag{22}$$

Thus, this equilibrium exists when

$$\frac{\mu_G \sigma_G}{S_G C_G} = \frac{\mu_B \sigma_B}{S_B C_B}. \tag{23}$$

However, this case is not biologically significant as it lies on the a boundary hyperplane of the parameter space. In the rare cases that (23) actually holds, the equilibrium exists. However, with any perturbation of the parameters, the condition no longer holds, so the equilibrium fails to exist. The same procedure can show the existence and insignificance of the Blue-Yellow Dimorphic Equilibrium, Orange-Yellow Dimorphic Equilibrium, and Orange-Blue-Yellow Trimorphic Equilibrium.

6 Acknowledgments

We would like to thank Dr. Carlos Castillo-Chavez, Executive Director of the Mathematical and Theoretical Biology Institute (MTBI), for giving us this opportunity to participate in this research program. We would also like to thank Summer Director Dr. Anuj Mubayi for his efforts in planning and executing the day-to-day activities of MTBI. This research was conducted in MTBI at the Simon A. Levin Mathematical, Computational and Modeling Sciences Center (SAL MCMSC) at Arizona State University (ASU). This project has been partially supported by grants from the National Science Foundation (DMS 1263374), the National Security Agency (H98230-15-1-0021), the Office of the President of ASU, and the Office of the Provost at ASU.

References

[1] Suzanne H Alonzo and Barry Sinervo. Mate choice games, context-dependent good genes, and genetic cycles in the side-blotched lizard, uta stansburiana. *Behavioral Ecology and Sociobiology*, 49(2-3):176–186, 2001.

[2] Malte Andersson and Leigh W Simmons. Sexual selection and mate choice. *Trends in Ecology & Evolution*, 21(6):296–302, 2006.

[3] Malte B Andersson. *Sexual selection*. Princeton University Press, 1994.

[4] Stavros Busenberg and Carlos Castillo-Chavez. Interaction, pair formation and force of infection terms in sexually transmitted diseases. In *Mathematical and statistical approaches to AIDS epidemiology*, pages 289–300. Springer, 1989.

[5] Carlos Castillo-Chavez, Wenzhang Huang, and Jia Li. On the existence of stable pairing distributions. *Journal of Mathematical Biology*, 34(4):413–441, 1996.

[6] Peter Chesson. Mechanisms of maintenance of species diversity. *Annual review of Ecology and Systematics*, pages 343–366, 2000.

[7] Ammon Corl, Alison R Davis, Shawn R Kuchta, and Barry Sinervo. Selective loss of polymorphic mating types is associated with rapid phenotypic evolution during morphic speciation. *Proceedings of the National Academy of Sciences*, 107(9):4254–4259, 2010.

[8] Charles Darwin and William F Bynum. *The origin of species by means of natural selection: or, the preservation of favored races in the struggle for life*. AL Burt, 2009.

[9] Klaus Dietz and KP Hadeler. Epidemiological models for sexually transmitted diseases. *Journal of mathematical biology*, 26(1):1–25, 1988.

[10] Terry L Erwin. An evolutionary basis for conservation strategies. *Science*, 253(5021):750, 1991.

[11] Marcus Frean and Edward R Abraham. Rock–scissors–paper and the survival of the weakest. *Proceedings of the Royal Society of London B: Biological Sciences*, 268(1474):1323–1327, 2001.

[12] Karl P Hadeler. Pair formation. *Journal of mathematical biology*, 64(4):613–645, 2012.

[13] Benjamin Kerr, Margaret A Riley, Marcus W Feldman, and Brendan JM Bohannan. Local dispersal promotes biodiversity in a real-life game of rock–paper–scissors. *Nature*, 418(6894):171–174, 2002.

[14] Robert M May and Warren J Leonard. Nonlinear aspects of competition between three species. *SIAM Journal on Applied Mathematics*, 29(2):243–253, 1975.

[15] Jeff Merckens, Bryce van de Geijn, Ioana Hociota, Donn Tadaya, and Benjamin Morin. The dynamics of a spatial cyclic competition system. *Mathematical and Theoretical Biology Institute*, 2009.

[16] Barry Sinervo, Benoit Heulin, Yann Surget-Groba, Jean Clobert, Donald B Miles, Ammon Corl, Alexis Chaine, and Alison Davis. Models of density-dependent genic selection and a new rock-paper-scissors social system. *The American Naturalist*, 170(5):663–680, 2007.

[17] Barry Sinervo and Curt M Lively. The rock-paper-scissors game and the evolution of alternative male strategies. *Nature*, 380(6571):240–243, 1996.

[18] Barry Sinervo, Donald B Miles, W Anthony Frankino, Matthew Klukowski, and Dale F DeNardo. Testosterone, endurance, and darwinian fitness: natural and sexual selection on the physiological bases of alternative male behaviors in side-blotched lizards. *Hormones and Behavior*, 38(4):222–233, 2000.

[19] Barry Sinervo, Erik Svensson, and Tosha Comendant. Density cycles and an offspring quantity and quality game driven by natural selection. *Nature*, 406(6799):985–988, 2000.

[20] Attila Szolnoki, Mauro Mobilia, Luo-Luo Jiang, Bartosz Szczesny, Alastair M Rucklidge, and Matjaž Perc. Cyclic dominance in evolutionary games: a review. *Journal of the Royal Society Interface*, 11(100):20140735, 2014.

[21] Donald W Tinkle. The life and demography of the side-blotched lizard, uta stansburiana. *University of Michigan Museum of Zoology*, 1967.